The synthesis, reactivity and modelling studies of [RuCl(CO)(η^2-C,O-C₆H₄-2-CHO)(PPh₃)₂]: Crystal and molecular structures of [RuCl(CO)(η^2-C,O-C₆H₄-2-CHO)(PPh₃)₂] · 3.5CHCl₃ and [Ru(NC^{t}Bu)(CO)(η^2-C,O-C₆H₄-2-CHO)(PPh₃)₂][BF₄] · 2CHCl₃

Kevin R. Flower *, Myles W. Garrould, Laura G. Leal, Claudia Mangold,
Patrick J. O'Malley, Robin G. Pritchard

School of Chemistry, The University of Manchester, Oxford Road, Manchester M13 9PL, UK

Abstract

Treatment of [RuHCl(CO)(PPh₃)₃] with Hg(C₆H₄-2-CHO)₂ in refluxing toluene gives [RuCl(CO)(η^2-C,O-C₆H₄-2-CHO)(PPh₃)₂] **1** in good yield. Treatment of **1** with a stoichiometric amount of Ag[BF₄] in CH₂Cl₂/acetone (1:1) followed by either NCMe, ^{t}BuCN or ^{t}BuNC to give [Ru(L)(CO)(η^2-C,O-C₆H₄-2-CHO)(PPh₃)₂][BF₄] **2–4** in excellent yields. All of the compounds **1–4** have been characterized by microanalysis, ¹H, ¹³C–{¹H} and ³¹P–{¹H} NMR spectroscopy. In addition compounds **1** and **3** have been characterized by single crystal X-ray diffraction studies and the cycloruthenated aldehyde C=O bond length noticeably increases in the cationic system. The complexes [RuCl(CO)(η^2-C,O-C₆H₄-2-CHO)(PH₃)₂] **1a**, [Ru(NCCH₃)(CO)(η^2-C,O-C₆H₄-2CHO)(PH₃)₂] **3a**, [Ru(CNCH₃)(CO)(η^2-C,O-C₆H₄-2CHO)(PH₃)₂] **4a** [RuCl₂{O=C(H)Me}(CO)(PH₃)₂] **Xa** and [RuCl₂{O=C(H)HCH=CH₂}(CO)(PH₃)₂] **XIa** have also been modelled using DFT calculations (B3LYP LanL2DZ) and the minimized structures are qualitatively in good agreement with experimentally determined structures. In all cases the calculated Ru–L distances were longer than those observed by experiment, the trend of Ru–C_(metalated) did not model the crystallographically observed data and some disparity between the experimental and calculated C=O bond length of the coordinated aldehyde is apparent.
© 2007 Elsevier B.V. All rights reserved.

Keywords: Ruthenium; Cyclometallation; Aldehyde; Crystal structure; Density functional theory

1. Introduction

Aldehydes are important reagents in the field of organic chemistry and much effort has been placed in developing their reactivity and this work continues a pace, in particular, the development of new catalytic systems to effect synthetically useful transformations [1]. Recent review articles are available on for example catalytic enantioselective addition of organometallic reagents [2] and the formyl CH···O hydrogen bond as a critical factor in enantioselec-

tive catalysis [3]. Few examples of cyclometallated aryl aldehydes are known. For example, Vicente and co-workers have used organomercurials as transfer reagents or oxidative addition of aryl bromides in the preparation of cyclopalladated aldehydes [4]. Other examples of *ortho*-formyl containing palladium complexes have been prepared by oxidative addition of aryltriflates [5]. Subsequent formyl group modification led to pincer complexes that were effective in Heck [6] and Michael reactions [7]. More recently Esteruelas et al. have effected *ortho*-C–H activation of benzaldehyde with [OsH₃(SnPh₂Cl){η^2-CH₂=C(CH₃)P^{i}Pr₂}(P^{i}Pr₃)] to give the cyclometallated complex [OsH₂(SnPh₂Cl){(η^2-C,O-C₆H₄-2-CHO)(P^{i}Pr₃)₂}] [8]. Other

examples of direct *ortho*-C–H activation are known [9]. The use of *ortho*-formyl halides in Stille [10] and Suzuki [11] cross coupling reactions have been described although the proposed *ortho*-palladated formyl complexes in the catalytic cycles were not isolated. An example of an *ortho*-formyl group having been prepared by ligand transformation reactions within the coordination sphere of palladium has also been described [12].

We recently reported a high yielding preparation of the diorganomercurial $Hg(C_6H_4-2-CHO)_2$ and its utility for the preparation of 2-phenyliminophenyls [13]. Herein we report its ability to transfer the benzaldehyde group to ruthenium using the methodology developed by Roper and Wright [14] and how ligand exchange can enhance the Lewis acidity of the ruthenium centre which manifests itself in crystallographically determined cycloruthenated benzaldehyde C=O bond lengths. Raman data for **4** suggest the $Cl_3CD\cdots F_2BF_2$ interaction is an example of a blue shifting hydrogen bond [15].

2. Results and discussion

Treatment of $[RuHCl(CO)(PPh_3)_3]$ with a stoichiometric amount of $Hg(C_6H_4-2-CHO)_2$ in refluxing toluene afforded $[RuCl(\eta^2-C,O-C_6H_4-2CHO)(CO)(PPh_3)_2]$ **1** in good yield along with elemental Hg, benzaldehyde and triphenylphosphine, Scheme 1. Compound **1** reacts with $Ag[BF_4]$ in CH_2Cl_2/acetone (1:1) which after filtration to remove precipitated AgCl reacts with NCMe, ^tBuCN and ^tBuNC to give the cationic complexes $[Ru(L)(\eta^2-C,O-C_6H_4-2-CHO)(CO)(PPh_3)_2][BF_4]$ **2–4** in excellent yield, Scheme 1. All of the compounds **1–4** have been characterized by elemental analysis, C, H and N, Table 1, ^1H, $^{31}P–\{^1H\}$ and $^{13}C–\{^1H\}$ NMR spectroscopy Tables 2 and 3. In addition compounds **1** and **3** have been characterized by single crystal X-ray diffraction studies, see Figs. 1 and 2 for ORTEP representations of the molecular structures of the cations, Tables 4 for crystal information and Table 5 for selected bond lengths (Å) and Table 6 for selected bond angles (°). Both structures, like that previously reported for **4** [15] are best considered as distorted octahedral about the central ruthenium atom with the two triphenylphosphine ligands axial with the CO ligand *trans* to the aldehyde oxygen atom in the equatorial plane. Both structures contain solvents of crystallization. For compound **1**, two of the chloroform solvates form non-conventional $Cl_3CH\cdots ClRu$ hydrogen bonds to the Cl(1), Fig. 3. This type of $Cl_3CH\cdots ClRu$ interaction was observed in the related complexes $[RuX(CO)(\eta^2-C,1N-C_6H_4CH=NC_6H_4-4R)-(PPh_3)_2]\cdot HCCl_3$ (X = F, Cl, Br, I; R = NO_2, Me) [16–18]. The non-conventional $Cl_3CH\cdots ClRu$ hydrogen bonds in **1** are shorter than those observed in $[RuX-(CO)(\eta^2-C,N-C_6H_4CH=NC_6H_4-4R)(PPh_3)_2]\cdot HCCl_3$ (X = F, Cl, Br, I; R = NO_2, Me) and this presumably results from less steric congestion about the Cl atom in the absence of the aromatic ring attached to the heteroatom allowing closer approach. For compound **3** like **4** [15] both chloroform solvates interact with the $[BF_4]^-$ counter anion giving rise to strong bifurcated $Cl_3CH\cdots F_2BF_2$ interactions, Fig. 4. Previously reported Raman data suggest this interaction is an example of an improper blue-shifting hydrogen bond [15].

A search of the CCDC [19] shows that there are only three other examples of crystallographically characterized complexes containing a chelating cyclometallated benzaldehyde ligand. The known complexes are $[OsH_2(SnPh_2Cl)(\eta^2-C_6H_4-2-CHO)(P^iPr_3)_2]$ **I** and $[OsH_2(SnPh_2Cl)(\eta^2-C_6H_4-2-CHO-6-OMe)(P^iPr_3)_2]$ **II** reported by Esteruelas et al. [8] and $ClHg(C_6H_4-2-CHO)$ **III** by Roper et al. [20]. Other structures that contain metallated aldehydes in the *ortho* position but not acting as a chelate ligand have been reported by Vicente et al. [4], Chart 1.

The aldehyde C=O moiety is seen to either point towards the Pd center **IV–VII** average $Pd\cdots O$ 2.9 Å with an average bond length of 1.212 Å or away from the Pd center **VIII–IX** with an average bond length of 1.211 Å which are comparable to the C=O bond length in **III** 1.208(13) Å. Clearly there is little deviation of the benzaldehyde C=O bond length in these complexes from that observed in uncoordinated systems [21]. In these cases, the metal centre is behaving as a weak Lewis acid. For **I** and **II** the aldehyde C=O bond length is elongated to 1.252(4) and 1.260(4) Å, respectively, showing a statistically supportable elongation in the C=O bond length implying that the osmium center is acting as a stronger Lewis acid than the metals in **III–IX** [8].

The closest related ruthenium complexes to **1–4** that have been crystallographically characterized are $[RuCl_2-\{\eta^1-O=C(H)C(Me)=C(H)Et\}(CO)(PPh_3)_2]$ **X** (C=O 1.242(4) Å) and $[RuCl_2\{\eta^1-O=C(H)^iBu\}(CO)(PPh_3)_2]$ **XI**

$$[RuHCl(CO)(PPh_3)_3] + Hg(C_6H_4-2CHO)_2$$

Scheme 1. (i) $C_6H_5CH_3$ reflux 6 h; (ii) $Ag[BF_4]$ CH_2Cl_2/acetone (1:1) 30 min. (iii) L 30 min.

Table 1
Analytical[a] and infra red[b] data for **1**–**4**

Compound	Yield (%)	Color	Analytical data	IR data (cm^{-1})
[RuCl(CO)(η^2-C,O-C$_6$H$_4$-2-CHO)(PPh$_3$)$_2$] · 3CHCl$_3$ **1**	77	Orange	C 48.8 (49.0) H 3.1 (3.3)	1920s v(C≡O) 1582m v(C=O)
[Ru(NCMe)(CO)(η^2-C,O-C$_6$H$_4$-2-CHO)(PPh$_3$)$_2$][BF$_4$]2CHCl$_3$ **2**	93	Yellow	C 51.4 (51.2) H 3.7 (3.6) N 1.1 (1.2)	2160w v(C≡N) 1953s v(C≡O) 1587m v(C=O) 1049bs v(B–F)
[Ru(NC^{t}Bu)(CO)(η^2-C,O-C$_6$H$_4$-2-CHO)(PPh$_3$)$_2$][BF$_4$]2CHCl$_3$ **3**	87	Yellow	C 52.6 (52.5) H 4.3 (4.0) N 1.1 (1.2)	2160w v(C≡N) 1954s v(C≡O) 1586m v(C=O) 1050bs v(B–F)
[Ru(CN^{t}Bu)(CO)(η^2-C,O-C$_6$H$_4$-2-CHO)(PPh$_3$)$_2$][BF$_4$]2CHCl$_3$ **4**	84	Pale yellow	C52.3 (52.5) H 4.1 (4.0) N 1.1 (1.2)	2179s v(C≡N) 1978s v(C≡O) 1585m v(C=O) 1051bs v(B–F)

 [a] Calculated in parentheses.
 [b] Spectra recorded as nujol mulls between KBr plates s = strong, m = medium, b = broad.

Table 2
Proton and ^{31}P{^{1}H} NMR data[a] for compounds **1**–**4**

Compound	^{31}P (δ)	^{1}H (δ)
1	35.5	8.80 (s, 1H, CHO); 7.50–7.10 (m, 30H, Ph–H); 7.07 (d, 1H, J_{HH} 7.8, Ph–H); 6.48 (t, 1H, J_{HH} 7.8, Ph–H); 6.21 (t, 1H, J_{HH} 7.8, Ph–H)
2	37.2	8.61 (s, 1H, CHO); 7.56–7.10 (m, 32H, Ph–H); 6.85 (m, 2H, Ph–H); 1.74 (s, 3H, NCCH$_3$)
3	37.2	8.71 (s, 1H, CHO); 7.48 – 7.03 (m, 32H, Ph–H); 6.85 (m, 2H, Ph–H); 0.85 (s, 3H, NCCCH$_3$)
4	37.3	8.64 (s, 1H, CHO); 7.52–7.05 (m, 32H, Ph–H); 6.90 (m, 2H, Ph–H); 0.94 (s, 3H, CNCCH$_3$)

 [a] Spectra recorded at 295 K in CDCl$_3$ and referenced to either H$_3$PO$_4$ (^{31}P) and CHCl$_3$ (^{1}H) coupling constants in Hz.

Table 3
^{13}C–{^{1}H} NMR data[a] for **1**–**4**

Compound	δ (ppm)
1	206.8[b] (t, J_{CP} 15.5, C≡O); 201.1 (s, C=O); 200.7[b] (t, J_{CP} 9.2, Ru–C$_{ar}$); 143.9[b]; 140.3; 134.3 (t, J_{CP} 5.8); 133.7; 131.9; 131.7[b] (vt, J_{CP} 23.0); 129.4; 127.7 (t, J_{CP} 4.8); 119.9
2[c]	203.9[b] (t, J_{CP} 13.8, C≡O); 202.9 (s, C=O); 195.4[b] (t, J_{CP} 8.9, Ru–C$_{ar}$); 144.7[b]; 140.2; 134.2; 133.9; 133.7 (t, J_{CP} 5.8); 130.8; 128.5 (t, J_{CP} 4.8); 128.2[b] (vt, J_{CP} 23.1); 121.9; 2.8
3	203.9[b] (t, J_{CP} 13.5, C≡O); 203.4 (s, C=O); 194.7[b] (t, J_{CP} 9.2, Ru–C$_{ar}$); 144.5[b]; 139.9; 135.1[b]; 134.5; 134.2; 133.4(t, J_{CP} 5.6); 130.9; 128.6 (t, J_{CP} 4.8); 128.4[b] (vt, J_{CP} 22.7); 122.2; 29.8[b]; 26.8
4[c]	205.5[b] (s, C=O); 203.5 (t, J_{CP} 12.6, C≡O); 198.6[b] (t, J_{CP} 9.6, Ru–C$_{ar}$); 145.1[b]; 139.4; 134.7; 134.3; 133.3(t, J_{CP} 5.1); 130.9; 128.6 (t, J_{CP} 4.5); 128.4[bd] (vt, J_{CP} 23.1); 122.9; 58.4[b]; 29.2

 [a] Spectra recorded in CDCl$_3$, coupling constants in Hz, t = triplet, v = virtual.
 [b] Quaternary carbon atoms identified by DEPT 135.
 [c] CN resonance not observed.
 [d] Partially obscured.

(C=O 1.234(4) Å) [1g]. A search of the CCDC [19] considering all TM–O=C(H)R bond lengths found 210 examples with well defined C=O bond lengths. In all but a handful of these cases the C=O bond length increased on complexation from the average C=O bond length in non-coordinated aldehydes, 1.192 Å [21]. The average C=O bond length is 1.232 Å with a median 1.230 Å, Fig. 5. A subset of these data were recently described in a study of η^1-O bound aldehydes at ruthenium [1g] and showed the shortest C=O bond to be 1.210 Å and the longest 1.263 Å with the mean 1.238 Å which compares favourably with all transition metal data. The bond lengths for **1**, **3** and **4**, are 1.233(5), 1.277(6) and 1.273(8) Å, respectively and fall within the in the defined range of all O-bound aldehyde-containing complexes, Fig. 5. For the cationic complexes **3** and **4** the C=O bond lengths are the longest yet observed for an aldehyde coordinated to a ruthenium centre and for **1** the bond length is comparable with other ruthenium aldehyde containing complexes [1g]. In this series of compounds the trend in the crystallographically determined C=O bond lengths is consistent with increasing the Lewis acidity at the metal increases the aldehyde C=O bond length, i.e. on going from a neutral to cationic metal centre.
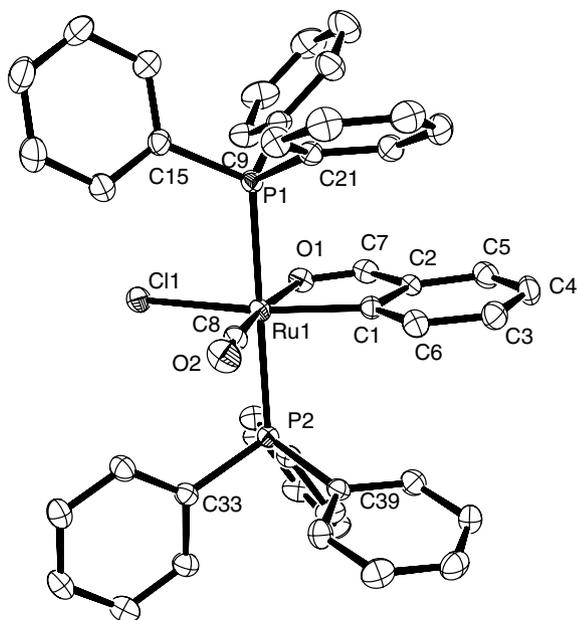
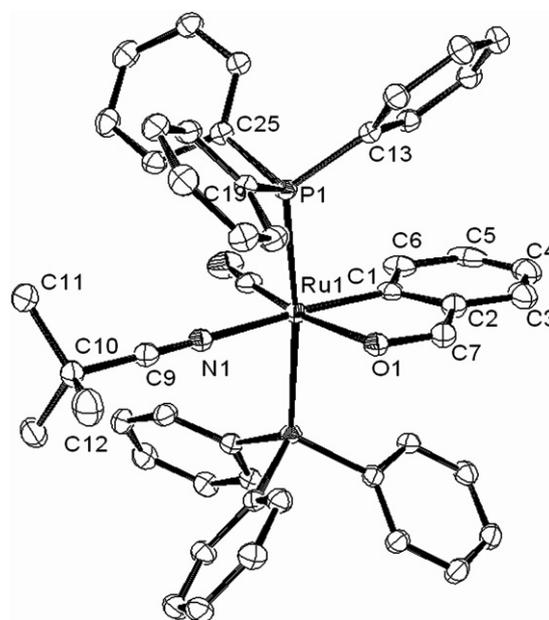Fig. 1. ORTEP representation of **1** showing the atomic numbering scheme. Ellipsoid probability at 30%.

Fig. 2. ORTEP representation of **3** showing the atomic numbering scheme. Ellipsoid probability at 30%.

In an attempt to see if this observed increase in C=O bond length with increasing Lewis acidity could be modelled, DFT calculations [22] (B3LYP LanL2DZ) on the model compounds $[RuCl(CO)(\eta^2\text{-}C,O\text{-}C_6H_4\text{-}2\text{-}CHO)\text{-}(PH_3)_2]$ **1a**, $[Ru(NCCH_3)(CO)(\eta^2\text{-}C,O\text{-}C_6H_4\text{-}2CHO)(PH_3)_2]$ **3a**, $[Ru(CNCH_3)(CO)(\eta^2\text{-}C,O\text{-}C_6H_4\text{-}2CHO)(PH_3)_2]$ **4a** were carried out. The data obtained were seen to be qualitatively in good agreement with the crystallographic data for **1**, **3** and **4**. However, the C=O bond length appeared to be more out of line than the other bond lengths, so the compounds $[RuCl_2\{O=C(H)HCH=CH_2\}(CO)(PH_3)_2]$ **Xa** and $[RuCl_2\{O=C(H)Me\}(CO)(PH_3)_2]$ **XIa**, which are simplifications of the crystallographically characterized compounds [1g] $[RuCl_2\{\eta^1\text{-}O=C(H)C(Me)=C(H)Et\}\text{-}(CO)(PPh_3)_2]$ **X** and $[RuCl_2\{\eta^1\text{-}O=C(H)^iBu\}(CO)(PPh_3)_2]$ **XI**, were also modelled. Selected bond lengths (Å) and angles (°) for **1a**–**XIa** can be found in Tables 5 and 6. The data for **Xa** and **XIa** were also qualitatively in good agreement with the experimental data. The major disagreement between the calculated and experimental structures is that the calculated bond lengths are, in all cases, slightly longer than the experimentally observed. This is common for this type of calculation and has been discussed by others elsewhere [23]. The calculated data for **Xa** and **XIa** suggest that for the α,β-unsaturated aldehyde there is a contribution of the resonance form **B**, Chart 2, to the overall structure which is not possible for the saturated aldehyde-containing complex **XIa** and accounts for the longer C=O bond and shorter Ru–O bond that are observed. A search of the CCDC [19] for $[(L_n)Ru(OR)]$ containing complexes shows a typical ruthenium alkoxide bond length of 2.0 (±0.05) Å and indicates there should be a significantly shorter Ru–O bond length in resonance form **B** and

supports the suggestion that **B** forms part of the overall structure. For **1a** the calculated Ru–O bond is comparable with **Xa** and for **3a** and **4a** it is shorter than for both **Xa** and **XIa** even though the *trans* ligand remains the same. From the experimental data it is reasonable to suggest that **1** has structural characteristics around the metallated aldehyde that are similar to the α,β-unsaturated aldehyde in **X** rather than the saturated aldehyde **XI**. This suggests a contribution to the overall structure **1** of resonance form **D** (Chart 1). The experimental data for **3** and **4** and the calculated structures for **3a** and **4a** show significant lengthening of the C=O bond of the aldehyde and a small reduction in the Ru–O bond lengths relative to **1** and **1a**. However these are within 3σ and may only indicate a trend which is consistent with enhanced Lewis acidity when considered in conjunction with the elongation of the C=O bonds in **3** and **4**. The crystallographically determined Ru–C$_{(met)}$ bond length increases **1** ≈ **3** < **4** and is mirrored in the calculations. The *trans* influence of a CNR ligand is considered to be comparable to CO [24] and greater than both Cl and NCR with experimental evidence suggesting that the *trans* influence of NCR is marginally weaker than Cl [25]. The trend in the crystallographically observed and calculated bond lengths for **1**, **3** and **4** supports this. The CNR ligand is also a significantly stronger π-acceptor than the metallated benzaldehyde implying the contribution of resonance form **D**, resulting from π-electron delocalization, to the observed structure for **4** is likely to be less than for **1** and **3**. The nitrile ligand has potential to be a weak π-acceptor through back donation into its π* orbitals, but the IR data show it is clearly a substantially weaker π-acceptor than CNR [25] leading to the expectation that the metal centre in **3** will be more electron rich (less Lewis

Table 4
Selected crystallographic data for **1** and **3**

	1	**3**
Empirical formula	$C_{47.5}H_{38.5}Cl_{11}O_2P_2Ru$	$C_{51}H_{46}BCl_6F_4NOP_2Ru$
F_w	1211.97	1167.48
T (K)	200 (2)	150 (2)
Crystal system	Triclinic	Orthorhombic
Space group	$P\bar{1}$	*Pnma*
a (Å)	9.7565 (2)	16.9432 (2)
b (Å)	10.29330 (10)	23.0386 (3)
c (Å)	26.2181 (5)	13.4180 (2)
α (°)	79.0080 (10)	90
β (°)	80.7310 (10)	90
γ (°)	88.4650 (10)	90
V (Å³)	2550.92 (8)	5237.69 (12)
Z	2	4
D_c (Mg m⁻³)	1.578	1.481
Crystal size (mm)	$0.20 \times 0.20 \times 0.08$	$0.22 \times 0.15 \times 0.07$
θ Range for data collections (°)	2.92–25.25	2.98–26.37
λ (Å)	0.71703	0.71703
Reflections collected	32977	39232
Unique reflections	9148	5473
Absorption correction	Semi-empirical from equivalents	Semi-empirical from equivalents
Largest difference between peak and hole (e Å⁻³)	0.604 and −0.740	1.441 and −1.053
Final R indices [$I > 2\sigma(I)$]		
R_1	0.0482	0.0480
wR_2	0.1035	0.1199
R indices all data		
R_1	0.0635	0.0619
wR_2	0.1133	0.1329
Data/restraints/parameters	9148/9/620	5473/0/433
Goodness-of-fit	1.044	1.052

Table 5
Selected crystallographic and calculated bond lengths (Å) for **1–XIa**

	1	**1a**	**3**	**3a**	**4** [15]	**4a**	**X** [1g]	**Xa**	**XI** [1g]	**XIa**
Ru–C(1)	2.037(4)	2.054	2.042(5)	2.055	2.086(6)	2.106				
Ru(1)–O(1)	2.162(3)	2.200	2.151(3)	2.162	2.157(4)	2.170	2.198(2)	2.203	2.211(2)	2.219
C(7)–O(1)	1.233(5)	1.285	1.277(6)	1.290	1.273(8)	1.289	1.242(4)	1.263	1.234(4)	1.256
C(7)–C(2)	1.436(5)	1.437	1.449(5)	1.435	1.457(10)	1.437	1.456(4)	1.463	1.469(5)	1.499
C(1)–C(2)	1.427(5)	1.447	1.412(7)	1.447	1.419(9)	1.445	1.341(5)	1.357	1.514(5)	
Ru(1)–Cl(1)	2.5059(10)	2.555					2.4235(9)	2.501	2.404(1)	2.499
Ru(1)–Cl(2)							2.3918(9)	2.478	2.383(1)	2.478
Ru(1)–C(9)					2.048(6)	2.066				
Ru(1)–N(1)			2.129(4)	2.229						
Ru(1)–P(1)	2.3940(10)	2.425	2.4027(7)	2.451	2.3979(10)	2.448	2.4115(8)	2.427	2.388(1)	2.427
Ru(1)–P(2)	2.3797(10)	2.424	2.4027(7)	2.453	2.3979(10)	2.448	2.3918(8)	2.427	2.396(1)	2.427
Ru(1)–C(8)	1.835(4)	1.843	1.852(5)	1.864	1.869(6)	1.870	1.842(4)	1.846	1.823(4)	1.844
C(8)–O(1)	1.133(5)	1.189	1.129(6)	1.189	1.119(7)	1.180	1.110(4)	1.184	1.138(4)	1.184

Table 6
Selected crystallographic and calculated angles (°) for **1–XIa**

|	**1**	**1a**	**3**	**3a**	**4** [9]	**4a**	**X** [1g]	**Xa**	**XI** [1g]	**XIa**
C(8)–Ru–O(1)	172.04(13)	173.55	167.95(19)	174.06	167.1(2)	173.74	179.0(1)	179.08	178.6(1)	179.46
P(1)–Ru–P(2)	176.67(4)	165.48	180	178.69	180	165.48	174.58(3)	175.64	178.33(4)	175.43
C(1)–Ru–L	163.71(11)	168.80	173.42(18)	170.52	174.9(2)	173.54				
Cl(1)–Ru–Cl(2)							168.56(3)	173.21	166.06(3)	173.08
Ru–C(1)–C(2)	113.3(2)	113.98	113.6(3)	112.92	113.0(4)	112.57				
C(1)–C(2)–C(7)	113.8(3)	114.94	114.8(4)	115.20	114.5(6)	115.28				
C(2)–C(7)–O(1)	121.5(4)	119.89	119.8(5)	119.50	120.6(6)	119.99	124.0(3)	121.46	124.7(4)	121.94
C(7)–O(1)–Ru	112.3(2)	112.67	112.4(3)	113.06	112.9(4)	113.86	130.0(2)	130.81	129.5(2)	130.81
O(1)–Ru–C(1)	78.87(12)	78.52	79.44(16)	79.32	79.1(2)	78.39				
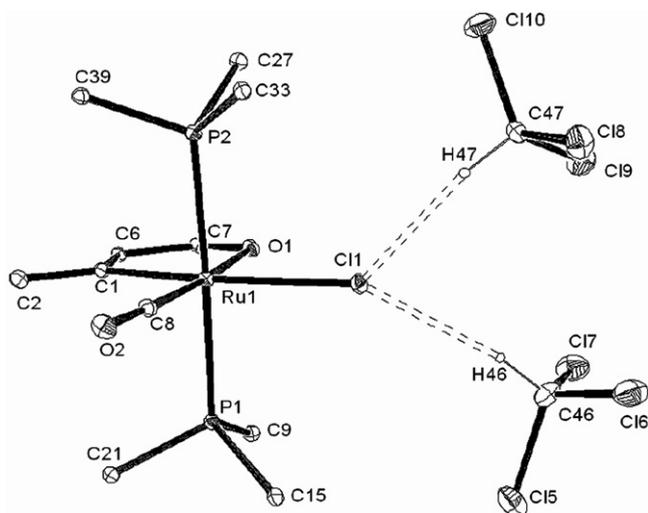
Fig. 3. ORTEP representation non-conventional Cl₃CH···ClRu hydrogen bonds observed in **1**. The phenyl rings are omitted for clarity with ellipsoid probability at 30%. C(46)–H(46) 0.999 Å, C(46)–H(46)···Cl(1) 2.596(2) Å, C(46)–Cl(1) 3.584(4) Å, C(46)–H(46)–Cl(1) 170.21(5)°; C(47)–H(47) 0.999 Å, C(47)–H(47)···Cl(1) 2.500(3) Å, C(47)–Cl(1) 3.460(5) Å, C(47)–H(47)–Cl(1) 161.01(5)°.
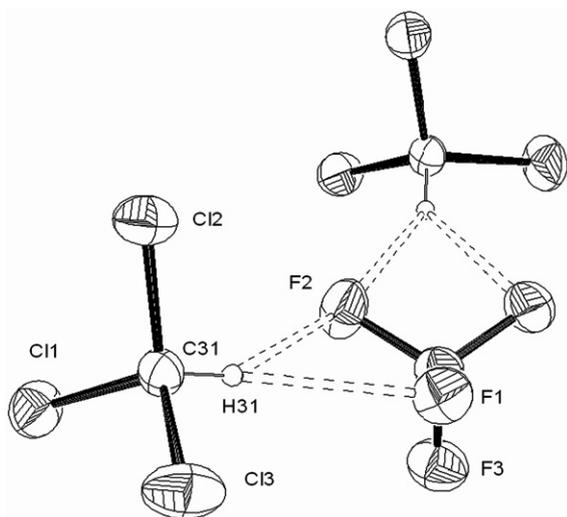
Fig. 4. ORTEP representation of the bifurcated Cl₃CH···F₂BF₂ interactions in **3**. Ellipsoid probability at 30 %. C(31)–H(31) 1.000(4) Å; H(31)···F(1) 2.372(3) Å; C(31)–H(31)···F(1) 144.30(3)°; H(31)···F(2) 2.314(3) Å; C(31)–H(31)···F(2) 152.45(2)°.

acidic) than **4** and therefore display shorter aldehyde C=O and longer Ru–O bond lengths. Experimentally, however, it is impossible to differentiate between the two. A plausible suggestion, for the complexes having the same bond lengths, is a greater contribution of resonance form **D** (Chart 1) to the structure of **3**, due to the reduced *trans* influence of NCR versus CNR, which would add to the effect of the enhanced Lewis acidity due to the metal centre being cationic in **3** and **4** and neutral in **1**.

The IR spectra for **1–4**, Table 1, all show a strong single ν(CO) band which shifts to higher wavenumbers for the cationic complexes, the highest as expected for **4** as it con-
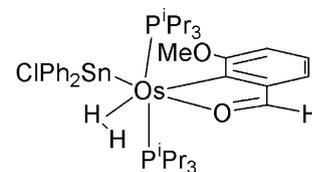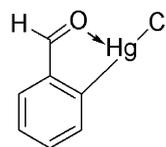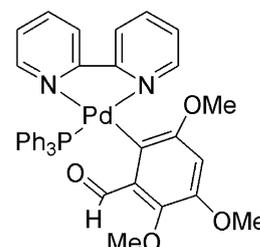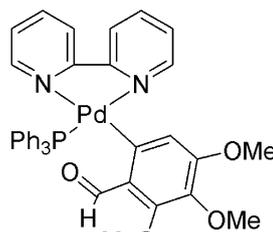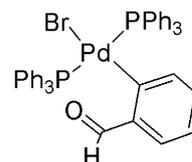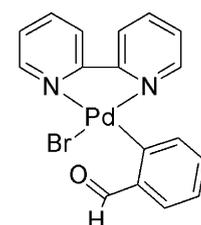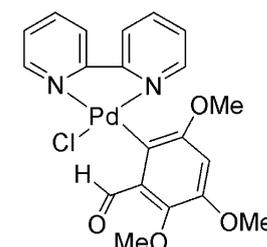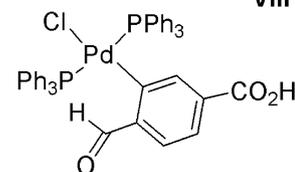
Chart 1.

tains a strong π-accepting isonitrile ligand. A strong ν(CN) band is also seen for the coordinated isonitrile ligand and in all cases the aldehyde ν(C=O) band shifts to below
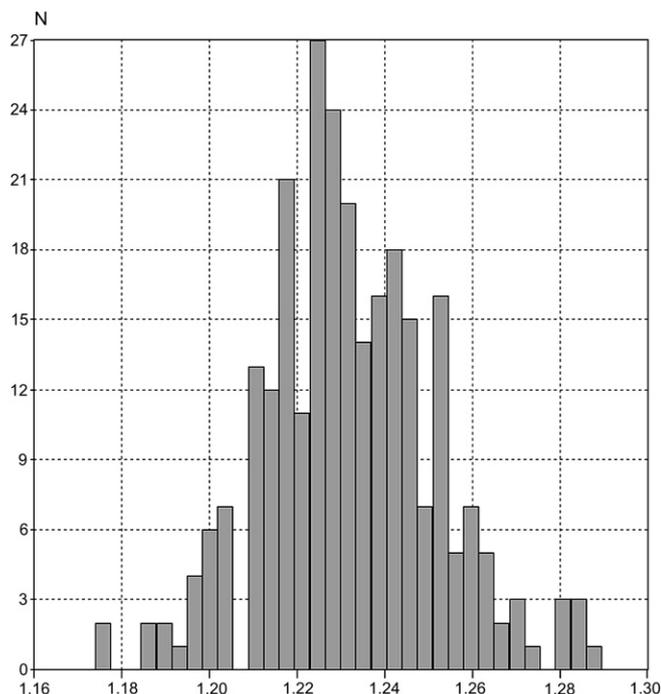
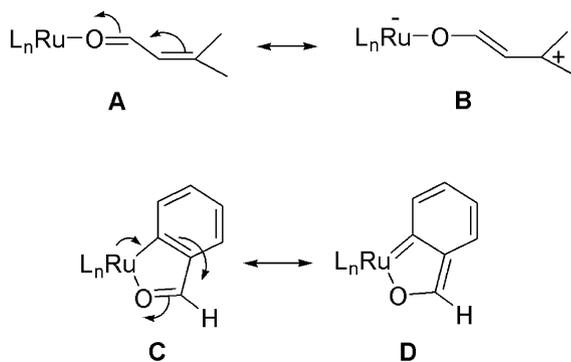Fig. 5. Histogram representation of the number of complexed aldehyde (C=O) bond lengths vs aldehyde C=O bond length.

Chart 2.

1600 cm^{-1} showing the expected reduction in the (C=O) bond order on complexation. The cationic complexes also display a strong v(BF) band at 1050 cm^{-1}. A Raman spectrum of **4** · 2CDCl$_3$ was recorded [15] to see if any information about the strength of the bifurcated hydrogen bond interaction Cl$_3$CH$\cdots$F$_2$ BF$_2$, observed in the solid state structure, could be obtained. The data suggest [15] that the bifurcated hydrogen bond interaction may be an example of an improper, blue-shifting hydrogen bond [26]. The solution state NMR data are consistent with the crystallographically determined solid state structures. The ^{31}P–{^{1}H} NMR spectra all show a singlet resonance, Table 2, which is consistent with the *trans* arrangement of the phosphine ligands. The proton spectra, Table 2, all show a singlet resonance for the cycloruthenated aldehyde proton: no evidence for coupling to the phosphorus nuclei was observed and is somewhat different from the related

complexes [RuCl(η^2-*C,N*-C$_6$H$_4$-2-CH=NC$_6$H$_4$-4-R)(CO)-(PPh$_3$)$_2$] (R = NMe$_2$, Me, I, NO$_2$) which display a small ca. 2 Hz coupling [27]. The proton spectra also show evidence for solvents of crystallization. On recrystallization from any halogenated solvent in the presence of Et$_2$O (see Section 4) incorporation of varying amounts of solvent of crystallization is obtained and analytical data needs to be carefully correlated with the proton data. Recrystallization from chloroform affords the most consistent analytical data for the cationic complexes. This is clearly due to the strong hydrogen bonding interaction, observed crystallographically, between the chloroform solvates and the [BF$_4$]$^-$ counter anion, Fig. 4. The ^{13}C–{^{1}H} NMR data are also consistent the formulation of **1**–**4**. The CO, RuC$_{ar}$ carbon resonances are clear triplets in the ^{13}C–{^{1}H} NMR spectrum (coupling to the two equivalent *trans* phosphine ligands) that disappear in the DEPT 135 spectrum. The higher frequency resonance has in all cases been assigned to the CO resonance and has the largest coupling constant. The metallated benzaldehyde carbon resonances for **1**–**4** (194.7–200.7 ppm) are comparable to those reported for the related cyclometallated osmium complexes **I** and **II** (198.2 and 200.3 ppm, respectively). Other analogues reported in the same paper had their metallated carbon atom resonance in this region too [8]. The CN resonances for the nitrile and isonitrile ligands in **2** and **4** respectively were not observed despite extend accumulation periods. It is possible that the CN resonance for **2** is obscured by one of the C$_{ar}$ resonances, this was nearly the case for **3**. For **4** the coupling to the two phosphorus atoms would reduce still further the signal to noise ratio of this quaternary carbon atom.

3. Conclusion

We have prepared a series of cycloruthenated benzaldehyde complexes which indicate that on going from a neutral to cationic system, effected by ligand exchange, the Lewis acidity of the metal centre is modified and that the change in the Lewis acidity manifests itself in the crystallographically determined C=O bond lengths of the aldehyde group. This observation is also supported by calculations on simplified model compounds. However, not all of the bond lengths around the cyclometallated ligand fit the expected pattern and this results from the different magnitudes of the *trans* effect.

4. Experimental

4.1. General considerations

All solvents, except alcohols, were dried by refluxing over an appropriate drying agent: toluene, sodium; CH$_2$Cl$_2$, P$_4$O$_{10}$; hexane and diethyl-ether, sodium–potassium alloy; and distilled prior to use. [RuHCl(CO)(PPh$_3$)$_3$] [28] and Hg(C$_6$H$_4$-2-CHO)$_2$ [13] were prepared according to the literature procedures. All other chemicals were

obtained from commercial sources and used as received except for $RuCl_3 \cdot 3H_2O$, which was loaned by Johnson Matthey. Infrared spectra were recorded as nujol mulls between KBr plates on a Nicolett 5PC spectrometer. Raman spectra were recorded in capillaries on a Nicolett Nexus spectrometer. ^1H NMR (200.2 MHz) and ^{31}P $\{^1H\}$ NMR (81.3 MHz) were recorded on a Bruker DPX200 spectrometer and ^{13}C $\{^1H\}$ NMR (100.55 MHz) were recorded on a Bruker DPX400 spectrometer. ^1H and ^{13}C $\{^1H\}$ NMR spectra were referenced to $CHCl_3$ ($\delta = 7.26$) and $CHCl_3$ ($\delta = 77.0$) and ^{31}P $\{^1H\}$ NMR were referenced externally to 85% H_3PO_4 ($\delta = 0.0$). Elemental analyses were performed by either the Microanalytical service, Department of Chemistry, UMIST, Manchester or School of Chemistry, The University of Manchester, Manchester; solvates of crystallization were confirmed by repeated elemental analysis and ^1H NMR. The syntheses of all complexes were carried out under a dinitrogen atmosphere using standard Schlenk techniques. Work-ups were generally carried out in the open unless otherwise stated.

4.1.1. [RuCl(CO)(η²-C,O-C₆H₄-2-CHO)(PPh₃)₂] · 2CHCl₃ 1

Caution: Use of an organomercurial. To [RuHCl-(CO)(PPh₃)₃] (1 g, 1.1 mmol) suspended in toluene (25 mL) was added [Hg(η²-C₆H₄-2-CHO)₂] (0.465 g, 1.15 mmol) and the solution refluxed under a continuous stream of dinitrogen for 6 h. After cooling to room temperature the solution was filtered through Celite to remove elemental Hg. The solvent was removed under reduced pressure and the crude material recrystallized from CH_2Cl_2/EtOH (0.68 g, 77%). Analytically pure material was obtained on recrystallization from chloroform. See Table 1 for physical and analytical data.

4.1.2. [Ru(NCMe)(CO)(η²-C,O-C₆H₄-2-CHO)(PPh₃)₂]-[BF₄] 2CHCl₃ 2

To 1 (0.08 g, 0.1 mmol) dissolved in acetone/CH_2Cl_2 (1:1, 10 mL) was added AgBF₄ (0.020 g, 0.1 mmol) and the solution stirred for 40 min. The solution was then filtered through a fluted filter paper and NCMe (2 mL) added and the solution stirred for 40 min, removal of the solvent in vacuo gave a yellow solid. Dissolution of this solid in CH_2Cl_2 (10 mL) and filtration through Celite removed remaining inorganic salts. Reduction of the solvent volume (2 mL) and drop-wise addition of Et₂O (10 mL) afforded 2 (0.083 g, 93%). Analytically pure material was obtained on recrystallization from chloroform. Compounds 3 and 4 were prepared in an analogous fashion. See Table 1 for physical and analytical data.

4.2. Crystallography

Crystals of 1 and 3 were grown by slow evaporation of a CHCl₃ solution at room temperature (20 mg in 1 mL). Data collections for 1 and 3 were carried out using ϕ and ω scans on a Nonius Kappa CCD diffractometer employing graphite monochromated Mo Kα radiation ($\lambda = 0.71073$ Å). Experimental details are described in Table 4. The crystal structures were solved by direct methods using SHELXS-97 and refined by full-matrix least-squares with SHELXL-97 [29].

Appendix A. Supplementary material

CCDC 663283 and 663284 contain the supplementary crystallographic data for this paper. These data can be obtained free of charge from The Cambridge Crystallographic Data Centre via www.ccdc.cam.ac.uk/data_request/cif. Supplementary data associated with this article can be found, in the online version, at doi:10.1016/j.jorganchem.2007.11.006.

References

[1] (a) A. Landa, A. Minkkilä, G. Blay, K.A. Jørgensen, Chem. Eur. J. 12 (2006) 3472;
(b) Y.-H. Chen, F.E. McDonald, J. Am. Chem. Soc. 128 (2006) 4568;
(c) J.T. Williams, P.S. Bahia, B.M. Kariuki, N. Spencer, D. Philip, J.S. Spencer, J. Org. Chem. 71 (2006) 2460;
(d) A.V. Kurdyumov, N. Lin, R.P. Hsung, G.C. Gullickson, K.P. Cole, N. Sydorenko, J. Swidorski, Org. Lett. 8 (2006) 191;
(e) L.-X. Shao, B. Xu, J.-W. Huang, M. Shi, Chem. Eur. J. 12 (2006) 510;
(f) L. Carosi, H. Lachance, D.G. Hall, Tetrahedron Lett. 46 (2005) 8981;
(g) A. Sorkau, C. Wagner, D. Steinborn, E. Poetsch, A.E.F. Wächtler, Trans. Met. Chem. 30 (2005) 691.
[2] S.E. Denmark, J. Fu, Chem. Rev. 103 (2003) 2763.
[3] E.J. Corey, T.W. Lee, Chem. Commun. (2001) 1321.
[4] (a) J. Vicente, J.-A. Abad, M.-A. Stiakaki, P.G. Jones, J. Chem. Soc., Chem. Commun. (1991) 137;
(b) J. Vicente, J.-A. Abad, B. López-Peláez, E. Martínez-Viviente, Organometallics 21 (2002) 58;
(c) J. Vicente, J.-A. Abad, E. Martínez-Viviente, M.C.R. de Arellano, Organometallics 19 (2000) 752;
(d) J. Vicente, J.-A. Abad, B. Rink, F.-S. Hernández, M.C.R. de Arellano, Organometallics 16 (1997) 5269;
(e) J. Vicente, J.-A. Abad, K.F. Shaw, J. Gil-Ribio, M.C.R. de Arellano, P.G. Jones, Organometallics 16 (1997) 4557;
(f) J. Vicente, J.-A. Abad, P.G. Jones, Organometallics 11 (1992) 3512.
[5] K. Takenaka, M. Minakawa, Y. Uozumi, J. Am. Chem. Soc. 127 (2005) 12273.
[6] K. Takenaka, Y. Uozumi, Adv. Synth. Catal. 346 (2004) 1693.
[7] K. Takenaka, Y. Uozumi, Org. Lett. 6 (2004) 1833.
[8] B. Eguillor, M.A. Esteruelas, M. Oliván, E. Oñate, Organometallics 23 (2004) 6015.
[9] F. Kakiuchi, T. Sato, K. Igi, N. Chatani, S. Murai, Chem. Lett. (2001) 386;
(b) R.C. Cambie, M.R. Metzler, P.S. Rutledge, P.S. Woodgate, J. Organomet. Chem. 398 (1990) C22;
(c) P.N. Robinson, L. Mann, B.K. Nicholson, J. Organomet. Chem. 349 (1988) 209.

[10] (a) O. de Frutos, A.M. Echavarren, Tetrahedron Lett. 37 (1996) 8953;
(b) O. de Frutos, C. Atienza, A.M. Echavarren, Eur. J. Org. Chem. (2001) 163.

[11] F.-J. Zhang, C. Cortez, R.G. Harvey, J. Org. Chem. 65 (2000) 3952.

[12] C. Fernandez-Rivas, D.J. Cardenas, B. Martin-Matute, A. Monge, E. Gutierrez-Puebla, A.M. Echavarren, Organometallics 20 (2001) 2998.

[13] K.R. Flower, V.J. Howard, S. Naguthney, R.G. Pritchard, J.E. Warren, A.T. McGown, Inorg. Chem. 41 (2002) 1907.

[14] W.R. Roper, L.J. Wright, J. Organomet. Chem. 142 (1977) C1.

[15] A.K. Brisdon, K.R. Flower, R.G. Pritchard, Inorg. Chem. 46 (2007) 7189.

[16] K.R. Flower, L.G. Leal, R.G. Pritchard, J. Organomet. Chem. 690 (2005) 3390.

[17] K.R. Flower, L.G. Leal, R.G. Pritchard, Inorg. Chem. Commun. 7 (2004) 729.

[18] K.R. Flower, R.G. Pritchard, J.E. Warren, Eur. J. Inorg. Chem. (2003) 1929.

[19] F.H. Allen, J.E. Davies, O.J. Johnson, O. Kennard, C.F. Macrae, E.M. Mitchell, G.F. Mitchell, J.M. Smith, D.G. Watson, J. Chem. Inf. Comput. Sci. 31 (1991) 187.

[20] C.E.F. Rickard, W.R. Roper, F. Tutone, S.D. Woodgate, L.J. Wright, J. Organomet. Chem. 619 (2001) 293.

[21] F.H. Allen, O. Kennard, D.G. Watson, L. Brammer, A.G. Orpen, R. Taylor, J. Chem. Soc., Perkin Trans. II (1987) S1.

[22] GAUSSIAN 03, Revision C.02, Gaussian, Inc., Wallingford, CT, 2004.

[23] E.A. McCullough, E. Apra, J. Nichols, J. Phys. Chem. A 101 (1997) 2502.

[24] (a) H.C. Clark, J.E.H. Ward, J. Am. Chem. Soc. 96 (1974) 1741;
(b) B.R. Steele, K. Vrieze, Trans. Met. Chem. 2 (1977) 140.

[25] F.D. Rochon, R. Melansom, E. Thouin, A.L. Beauchamp, C. Bensimon, Can. J. Chem. 74 (1996) 144.

[26] (a) P. Hobza, Z. Havlas, Chem. Rev. 100 (2000) 4253;
(b) B.J. van der Veken, W.A. Herrebout, R. Szostak, D.N. Shchepkin, Z. Havlas, P. Hobza, J. Am. Chem. Soc. 123 (2001) 12290;
(c) H. Sato, J. Dybal, R. Murakami, I. Noda, Y. Ozaki, J. Mol. Struct. 744–747 (2005) 35.

[27] K.R. Flower, V.J. Howard, R.G. Pritchard, J.E. Warren, Organometallics 21 (2002) 1184.

[28] N. Ahmad, J.J. Levison, S.D. Robinson, M.J. Uttley, Inorg. Synth. 15 (1974) 48.

[29] G.M. Sheldrick, SHELX-97 Program Package; University of Goettingen, 1997.